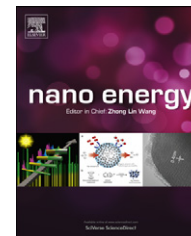


Available online at www.sciencedirect.com

SciVerse ScienceDirect

journal homepage: www.elsevier.com/locate/nanoenergy

RAPID COMMUNICATION

Silicon-conductive nanopaper for Li-ion batteries

Liangbing Hu^{a,1}, Nian Liu^{b,1}, Martin Eskilsson^{d,e,1}, Guangyuan Zheng^c, James McDonough^a, Lars Wågberg^{d,e,**}, Yi Cui^{a,f,*}^aDepartment of Materials Science and Engineering, Stanford University, Stanford, CA 94305, USA^bDepartment of Chemistry, Stanford University, Stanford, CA 94305, USA^cDepartment of Chemical Engineering, Stanford University, Stanford, CA 94305, USA^dDepartment of Fibre and Polymer Technology, Royal Institute of Technology (KTH), Teknikringen 56, 10044 Stockholm, Sweden^eWallenberg Wood Science Centre, Royal Institute of Technology (KTH), Teknikringen 56, 10044 Stockholm, Sweden^fStanford Institute for Materials and Energy Sciences, SLAC National Accelerator Laboratory, 2575 Sand Hill Road, Menlo Park, CA 94025, USA

Received 17 July 2012; received in revised form 14 August 2012; accepted 15 August 2012

KEYWORDS

Li-ion battery;
Silicon anode;
Conductive aerogel;
Aqueous ink;
Cellulose fibrils;
Low cost

Abstract

There is an increasing interest in the development of thin, flexible energy storage devices for new applications. For large scale and low cost devices, structures with the use of earth abundant materials are attractive. In this study, we fabricated flexible and conductive nanopaper aerogels with incorporated carbon nanotubes (CNT). Such conductive nanopaper is made from aqueous dispersions with dispersed CNT and cellulose nanofibers. Such aerogels are highly porous with open channels that allow the deposition of a thin-layer of silicon through a plasma-enhanced CVD (PECVD) method. Meanwhile, the open channels also allow for an excellent ion accessibility to the surface of silicon. We demonstrated that such lightweight and flexible Si-conductive nanopaper structure performs well as Li-ion battery anodes. A stable capacity of 1200 mA h/g for 100 cycles in half-cells is achieved. Such flexible anodes based on earth abundant materials and aqueous dispersions could potentially open new opportunities for low-cost energy devices, and potentially can be applied for large-scale energy storage.

© 2012 Elsevier Ltd. All rights reserved.

*Corresponding author at: Department of Materials Science and Engineering, Stanford University, Stanford, CA 94305 USA.

**Corresponding author at: Department of Fibre and Polymer Technology, Royal Institute of Technology (KTH), Teknikringen 56, 10044 Stockholm, Sweden

E-mail addresses: wagberg@kth.se (L. Wågberg), yicui@stanford.edu (Y. Cui).¹These authors contributed equally to this work.

Introduction

There is a strong interest in developing flexible, lightweight energy storage devices to meet the various power needs of consumer electronics and military devices. Recently, there are a few demonstration devices on this topic, including nanocomposite paper storage devices, flexible Li-ion batteries with paper as a mechanical support and a separator, supercapacitors

2211-2855/\$ - see front matter © 2012 Elsevier Ltd. All rights reserved.
<http://dx.doi.org/10.1016/j.nanoen.2012.08.008>Please cite this article as: L. Hu, et al., Silicon-conductive nanopaper for Li-ion batteries, Nano Energy (2012), <http://dx.doi.org/10.1016/j.nanoen.2012.08.008>

with conductive polymers and others [1-7]. For low-cost applications, earth abundant materials are preferred. Cellulose is the most abundant natural polymer on earth and Si is the second most abundant element in the earth's crust. Cellulose has been widely used as a key component in flexible devices and usually as mechanical support or templates for achieving porous nanostructures [8].

Silicon is an attractive alloy-type anode material because of its highest known capacity (4200 mA h/g). However, lithium insertion into and extraction from silicon are accompanied by a huge volume change (up to 400%), which induces a strong stress on the silicon particles and causes pulverization and rapid capacity fading [9,10]. To overcome this issue, several approaches have been suggested, including the preparation of nano-sized active materials, active/inactive composite materials and Si-based carbon composites [11-18]. Recently, cellulose-graphite nanocomposites have been demonstrated as a flexible electrode for Li-ion batteries [19]. However, the use of graphite limits the overall capacity of the electrode. The use of Si in this structure will largely enhance the capacity of flexible Li-ion batteries.

On the other side, manipulations of electrons and ions to allow for the fast transport are important for high-rate performances in energy storage devices. Structures with tunable open channels are attractive for this purpose. Recently, conductive aerogels have been demonstrated with carbon nanotubes (CNT). The aerogel shows excellent mechanical properties [20,21]. Such structures provide an excellent platform for fast ion transport. However, these structures have not been explored for flexible Li-ion batteries. In this work we fabricate conductive CNT-cellulose aerogels that are coated with Si by a plasma-enhanced CVD (PECVD) method. Such nanocomposites were evaluated as a flexible anode for Li-ion batteries. We also compare their performance with that of a structure where Si is deposited on CNT-regular paper fibers. Excellent performance as a Li-ion battery anodes have been demonstrated, which is promising for flexible electronics. As the materials are potentially low cost and the processes are scalable, the structure demonstrated in this work could also be useful for large-scale energy storage.

Materials and methods

Carboxymethylated nanofibrillated cellulose (NFC) preparation

Carboxymethylated nanofibrillated cellulose was kindly provided by Innventia AB (Stockholm, Sweden) and fabricated using a method previously described by Wågberg et al. [25]. The never-dried softwood dissolving fibres (Domsjö Fabriker AB, Domsjö, Sweden) were subjected to a carboxymethylation and a subsequent homogenization using a high-pressure homogenizer (Microfluidizer M-110EH, Microfluidics Corp.) [25].

To start with, the fibres were dispersed in deionized water using a laboratory mixer at 10,000 revolutions followed by a solvent exchange with ethanol. This was followed by the actual carboxymethylation step comprising of an impregnation with 2% w/w of monochloroacetic acid dissolved in isopropanol. Following carboxymethylation, the fibres were filtered and washed with deionized water/ acetic acid/ deionized water followed by a conversion of the carboxyl groups to their sodium

form using a 4% w/w NaHCO₃ impregnation. The fibers were then washed with deionized water in order to remove excess salt and then subject to homogenization by being passed through the high-pressure homogenizer. Typically, NFC of 2% w/w concentration was then obtained.

Preparation of NFC:CNT dispersion

6.6 g of NFC of 2.17% w/w concentration was diluted with 50 mL deionized water to form a 0.28% w/w solution followed by 10 min homogenization using a T18 Basic Ultra Turrax (IKA) at 12,000 RPM. Then 10 mL of a P3 single-walled CNTs (Carbon Solutions, Inc.) dispersion with a concentration of 6.6 mg/mL was added to the mixture. This dispersion was prepared by first diluting 66 mg of CNTs in 10 mL of 1% w/w Triton-X 100 in deionized water followed by a sonication for 10 min at 20% amplitude using a VibraCell (Sonics & Materials, Inc.).

After an additional 20 min of mixing, 450 μ L of 200 mg/mL of polyvinylamine (BASF) was added thereby yielding a polyvinylamine content of 2 mg/g NFC. The mixture was subsequently stirred for 10 min. This procedure was used to improve the wet integrity of the NFC:CNT aerogel.

Fabrication of the NFC: CNT aerogel

The obtained NFC:CNT slurry was then subject to dewatering to a certain extent in order to reach a desired porosity. This was achieved using a simple and convenient vacuum filtration method in which the slurry was vacuum filtered on a 0.1 μ m mixed cellulose ester (MCE) membrane filter (Millipore) using a PG90 glass filter setup (Advantec MFS, Inc.) for 2 h at room temperature. This yielded a circular and uniform hydrogel with a diameter of 72 mm.

The obtained hydrogel was then transferred to an aluminum mold and rapidly frozen by dipping into liquid nitrogen for 2 min. The sample was then placed in a conventional freeze-dryer at -50°C and 50 μ bar for 24 h to ensure a proper drying without collapsing the structure. Finally, the obtained aerogel was heat-treated for 30 min at 140°C using a vacuum oven in order to induce cross-linking and hence to improve the web strength.

Fabrication of the regular paper based on paper pulp

Regular paper sheets were fabricated using a semi-automatic sheet former (Rapid-Köthen, PTI, Vorchdorf, Austria). First of all, softwood dissolving pulp was soaked for 4 h followed by mixing in an ordinary laboratory mixer (Disintegrator, Frank-PTI). The pulp suspension was then dewatered using the sheet former. The paper formed on top of the forming wire was then removed and stacked in between two paper sheets and placed in a sheet drier for 15 min at 93°C and 70 mbar. This yielded a paper with a diameter of 20 cm and grammage of approximately 100 g/m².

CNT coating on regular paper

CNT was applied on the paper surface using a method developed earlier by us [31]. To start with, an aqueous

CNT ink of 1 mg/mL in 1 w/w% sodium dodecyl benzene sulphonate (SDBS) in DI water was used as the coating material. The CNT ink was then applied onto the paper surface using manual Meyer rod coating followed by drying in a vacuum oven at 100 °C for 10 min. This yielded a uniform CNT coating on the paper.

Cell fabrication and electrochemical performance testing

The Si-conductive nanopaper was heated in vacuum oven at 100 °C for 3 h prior to cell fabrication. Coin-type cells (2032) were fabricated inside Ar-filled glovebox using Si-conductive nanopaper, Li metal foil, and Celgard 2250 separator soaked in self-made electrolyte. No binders or carbon black was used. The electrolyte was 1.0 M LiPF₆ in 1:1 w/w ethylene carbonate/diethyl carbonate (EMD Chemicals). 3 vol% fluoroethylene carbonate (Novolyte Technologies) was added to the electrolyte to improve the cycling stability of Si. The mass of Si was calculated by the area of the electrode and the PECVD deposition thickness. The capacity is calculate based on the mass of Si only. All electrochemical measurements were made using a Biologic VMP3 battery tester. The voltage cutoffs are 0.01 and 1 V vs Li/Li⁺. The rate, if not mentioned otherwise, was C/5 in terms of the theoretical capacity of Si (4200 mA h/g). Pouch-type cell is fabricated and tested for the Si-regular paper sample. In impedance measurements, the explored frequency range was from 100 mHz to 100 kHz under ac stimulus with 5 mV of amplitude and no applied voltage bias.

Results and discussion

Manipulations of ions and electrons in electrode materials are important for high-rate performance. Therefore, it is crucial to create a structure that is both porous for fast ion movement and electrically conductive with percolative

pathways. Aerogel created by freeze-drying method is typically porous with open channels for fast ion transport [22]. In the aerogel prepared in the present work, one-dimensional materials, NFCs and CNTs, are used. These two materials are with very similar dimensions, having a diameter of a few nanometers and a length in the order of micrometers. Figure 1(a) shows the schematic of the nanocomposites where CNTs are interwoven with NFCs. CNTs have a very low percolation threshold due to their 1D structure [23,24]. This ensures the excellent electrical conductivity of the nanocomposite. Therefore, a structure that has excellent transport for electrons and ions is obtained. We applied a low-temperature PECVD method for the Si deposition, which is compatible with the aerogel. Such gas-based deposition method allows the conformal coating of the Si. Therefore, the porous structure is maintained (Figure 1(b)). The NFC in our structure can also allow the volume expansion of silicon by functioning as a mechanical buffer. Note that the conductive nanopaper before Si deposition is made of interpenetrated 1D nanomaterials, including CNT and NFC that have very similar dimension in length and diameter (Figure 1(c)).

To fabricate the conductive and porous nanopaper aerogel, aqueous ink with CNTs and NFCs are made separately. The experiment details can be found in the Materials and methods section. These two types of aqueous ink are compatible. NFC was fabricated using a method previously described by Wagberg et al. [25]. Figure 2(a) shows the NFC:CNT aqueous slurry. For the fabrication of NFC:CNT aerogel, the NFC:CNT slurry was then subject to dewatering to a certain extent in order to reach a desired porosity. This was achieved using a simple and convenient vacuum filtration method (Figure 2(b)). The hydrogel was then transferred to an aluminum mold and rapidly frozen in liquid nitrogen for 2 min. Following freezing, the sample was placed in a conventional freeze-dryer for 24 h to ensure a proper drying without collapsing the structure. Finally, the obtained aerogel was heat-treated using a vacuum oven in

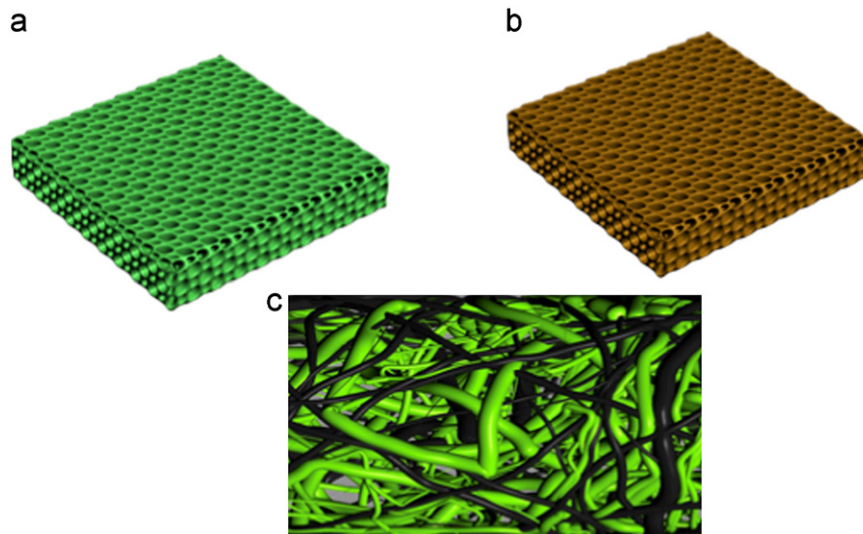


Figure 1 Schematic of Si-conductive nanopaper anode. (a) Zoom-in of conductive nanopaper with CNTs and NFCs. (b) Conductive nanopaper overcoated with a thin layer of Si by low-temperature PECVD process. (c) NFC:CNT nanocomposites with percolative pathways for electron transport. The blacks lines are CNTs and the green lines are NFCs.

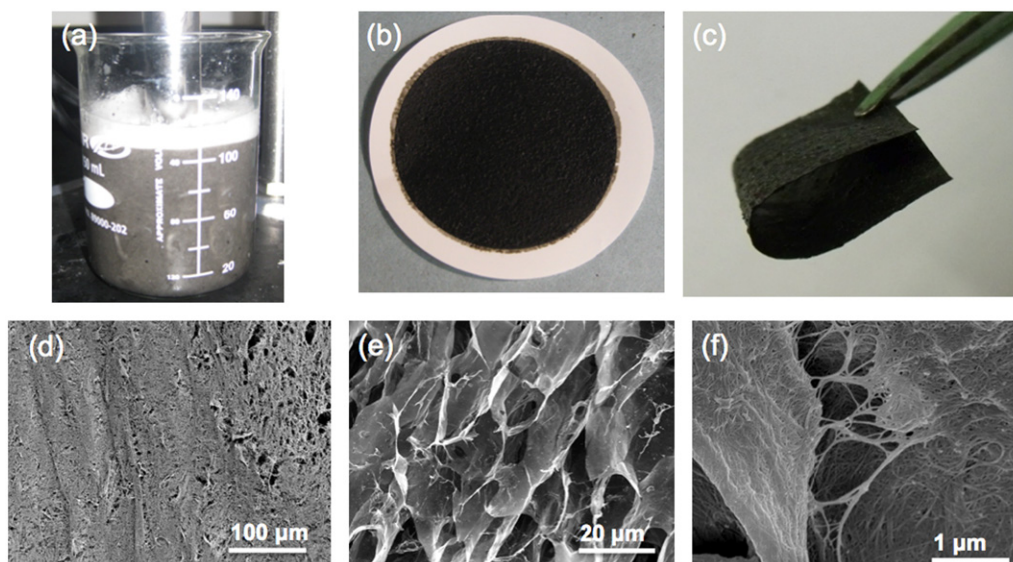


Figure 2 Fabrication of conductive, flexible nanopaper aerogel. (a) Aqueous dispersion of CNTs and nanocellulose fibers. (b) A web film made of slurry in (a). (c) A freeze-dried conductive nanopaper (~200 μm thick). (d)-(f) SEM of conductive nanopaper with different magnification.

order to induce cross-linking and hence improve web strength. The final film was mechanically flexible and could be cut into different shapes and sizes (Figure 2(c)). The typical sheet resistance of the NFC:CNT aerogel is $\sim 80 \Omega/\text{sq}$. The sheet resistance of aerogel could be tailored with different CNT density by a few magnitudes as in other conductive polymer-CNT composites [24-26].

The NFC:CNT aerogel is highly porous as shown in Figure 2(d)-(e). This highly porous structure is important for several reasons. The porous structure allows the excellent PECVD deposition of Si on the surface, which decreases the thickness of the films for a given areal mass. The smaller thickness of Si film allows faster kinetics inside the electrode film, which is crucial for high electrode performance at a high charge-discharge rate. On the other hand, the open and porous channels allow for a fast transport of ions in the electrolyte into the electrode materials. In a magnified SEM image in Figure 2(f), an interwoven structure with 1D CNT and NFC fibers is visible. Such conductive nanopaper shows an open structure due to the freeze-drying process.

A range of materials can be deposited on the porous, conductive nanopaper for the use as battery electrodes. The process temperature of conductive nanopaper is very limited ($< 150^\circ\text{C}$). PECVD is widely used for solar cell manufacturing in industry for Si deposition. Figure 3(a) shows a conductive nanopaper after a thin layer of PECVD deposition. After the deposition, the conductive nanopaper is still highly flexible (Figure 3(b)). Since the thickness of Si is much smaller compared with the pore size, the porous structure is maintained (Figure 3(c)). The fibrous structure of the nanopaper is maintained at the micro scale (Figure 3(d) and (e)). Nitrogen adsorption (Brunauer-Emmett-Teller, BET) measurements indicated that the specific surface area of the nanopaper aerogel is $41.3 \text{ m}^2/\text{g}$, the average pore size is 12.7 nm and the pore volume is $0.12 \text{ cm}^3/\text{g}$. The silicon mass, $0.046 \text{ mg}/\text{cm}^2$, was estimated from the thickness of PECVD deposition.

Electrochemical performance of this type of Si-conductive nanopaper was tested using coin-type cells with Li metal as the counter/reference electrode. During galvanostatic cycling with a current density of $0.8 \text{ A}/\text{g Si}$ (C/5), the Si-conductive nanopaper shows typical voltage profiles of amorphous Si lithiation/delithiation (Figure 4(a)). Mainly due to the initial formation of solid electrolyte interphase (SEI) and other side reactions, the first charge has a specific capacity of $\sim 5000 \text{ mA h}/\text{g Si}$, which is beyond the theoretical value ($4200 \text{ mA h}/\text{g}$). The first discharge reveals the reversible capacity to be $\sim 2100 \text{ mA h}/\text{g}$, which is similar to the reported values for amorphous Si [18-27]. This number is more than 5 times of the theoretical capacity of graphite anodes. After the first cycle, the voltage profile becomes more reversible. The second and tenth discharge profile almost overlaps and the 100th discharge profile is also very close to the second and the tenth. It is noted that the initial Coulombic Efficiency (CE) is low (43%), which may be due to the side reactions on functional groups on CNTs in the nanopaper at very low potential ($< 0.3 \text{ V}$ versus Li^+/Li). The low CE could be overcome by surface modification of the CNTs or by prelithiation of the Si-conductive nanopapers using a previously reported method [17].

The cycle stability of Si-conductive nanopapers is high as shown in Figure 4(b). After 100 deep charge/discharge cycles, the discharge capacity still remains 83% compared to the second cycle and 77% compared to the first cycle. After 100 cycles, the capacity still remains above $1200 \text{ mA h}/\text{g}$, which is more than 3 times the theoretical capacity of graphite, the currently used anode material. The stable cycling of Si-conductive nanopaper could possibly be due to three reasons. First, the 3D porosity in sub-micrometer scale allows the silicon to release the strain built up during repetitive lithiation/delithiation. Si expands 400% during lithiation and our design of this porous structure has enough empty spaces inside and therefore improves the cycle stability. Second, the mechanical flexibility of the conductive framework made of NFC and CNT further accommodates the volume change of Si by changing its shape. Compared to

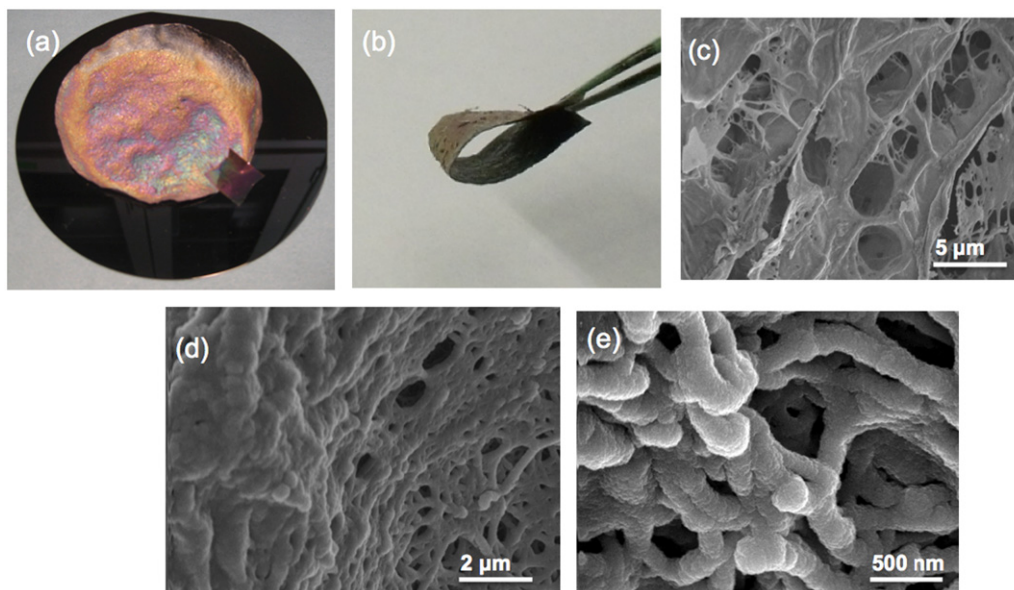


Figure 3 Si coating on conductive, flexible nanopaper aerogel. (a) A picture of conductive nanopaper coated with Si sitting on a silicon wafer. The thickness of Si coating is controlled by the PECVD deposition time. (b) The bent Si-conductive nanopaper to demonstrate the mechanical flexibility. (c)-(e) show the surface morphology at different magnification.

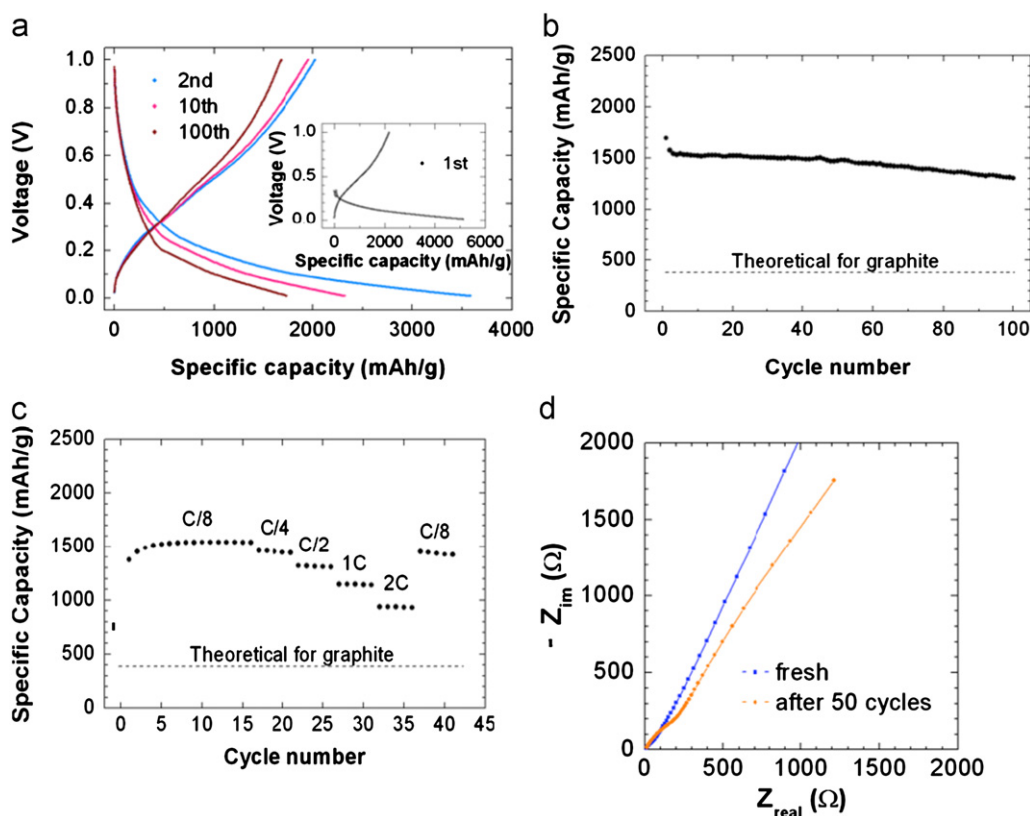


Figure 4 Electrochemical characterization of Si-conductive nanopaper with Li metal as the counter/reference electrode. (a) Voltage profiles of selected galvanostatic cycles. The voltage range is 0.01-1 V and the current density is 0.8 A/g Si (C/5). The numbers indicate the voltage profiles for different cycles. (b) Cycling performance of the discharge (delithiation) capacity of the half cell. (c) Electrochemical impedance of the half cell before cycling and after 50 cycles. (d) Rate performance of the half cell with different charge/discharge rates.

incompressible metal foil substrate/current collector, the conductive nanopaper is highly flexible due to the flexible nature of CNT and NFC. This can be seen from the flexibility

test shown in Figure 2(c). Third, the use of fluoroethylene carbonate (FEC) additive helps form a relatively stable solid-electrolyte-interphase (SEI) on the surface of Si [28], therefore

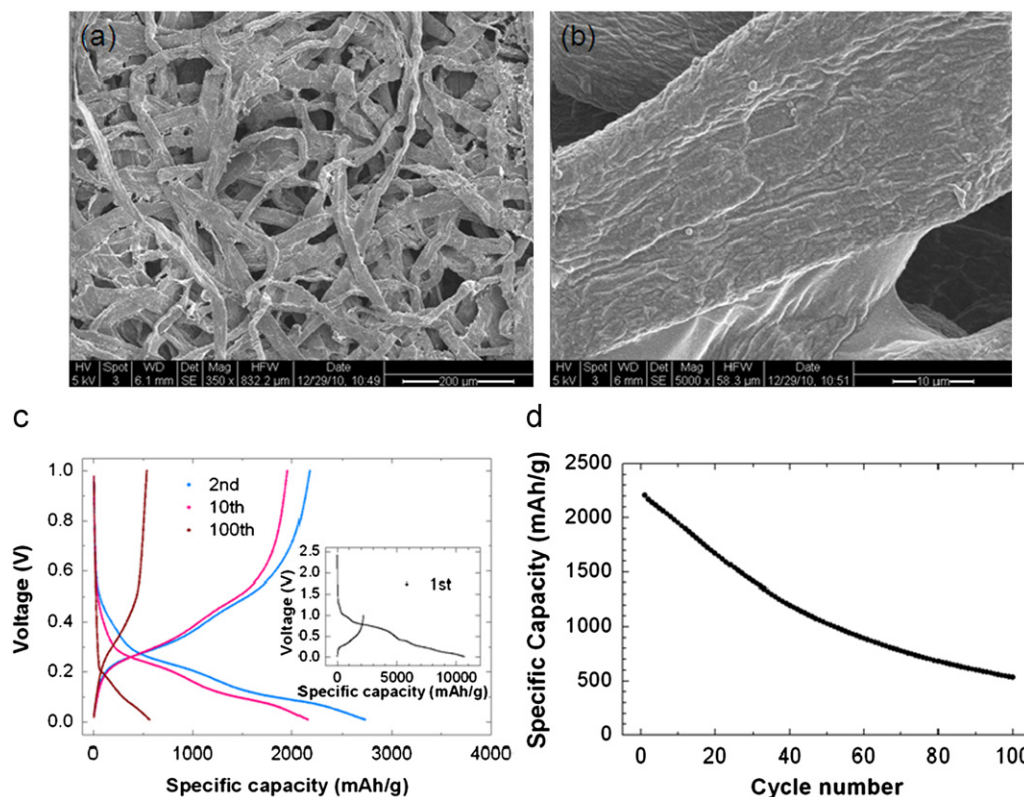


Figure 5 Characterization and electrochemical performance of Si thin film on conductive regular paper. (a) SEM of conductive regular paper after Si deposition. The size of fiber is $\sim 20\ \mu\text{m}$. (b) Zoom-in SEM of one paper fiber in (a). (c) Voltage profiles of selected galvanostatic cycles. The voltage range is 0.01–1 V and the current density is 0.8 A/g Si (C/5). (d) Cycling performance of the discharge (delithiation) capacity for the half cell.

ensures the reversible lithiation/delithiation process and minimizes active material loss. A stable SEI grown on the surface of Si will prevent the further decomposition of electrolyte while still allowing Li ions to migrate through without too much impedance. To monitor the SEI growth over cycling, an electrochemical impedance spectroscopic (EIS) analysis was carried out [29]. As depicted in the Nyquist plot in Figure 4(d), the spectrum after 50 deep galvanostatic cycles is very similar to the one before cycling, indicating that the SEI on the Si-conductive nanopaper is thin and stable. This kind of SEI could contribute to the stable cycling.

The Si-conductive nanopaper maintains high capacity at higher rate. As shown in Figure 4(c), galvanostatic cycling was performed at various C rates. Even at 2C rate (30 min charge/discharge), the capacity is still $\sim 1000\ \text{mA h/g}$, more than twice the theoretical capacity of graphite. The capacity remains 62% from C/8 to 2C, while the current density increases 16 times. This good rate capability is due to the 3D porous conductive framework, which allows fast transport for Li ions and electrons.

To study the effect of 3D submicrometer porosity on the cell performance, we tested the galvanostatic cycling of Si deposited directly on CNT coated regular paper (Si-regular paper). The morphology of Si-regular paper is shown in the SEM images in Figure 5(a) and (b). Regular paper was fabricated based on paper pulp using a filtration method and is made of cellulose fibers with a diameter of $\sim 20\ \mu\text{m}$ and a length of $\sim 2\ \text{mm}$ (see Materials and methods section for detailed fabrication method). The voltage profiles of

Si-regular paper are shown in Figure 5(c). In the first cycle, there is a large irreversible capacity, probably due to the SEI formation and side reactions on CNTs. The first discharge capacity is $\sim 2000\ \text{mA h/g}$ Si, close to the value of Si-conductive nanopaper, which means the deposited Si has been fully reacted with Li and the reaction is reversible. However, the cycle stability of Si-regular paper is poor compared to the Si-conductive nanopaper. After 100 cycles (Figure 5(d)), only $\sim 550\ \text{mA h/g}$ discharge capacity is retained, which is $\sim 25\%$ of the initial capacity. Compared to the 77% capacity retention of Si-conductive nanopaper, the cycle stability of Si-regular paper is much worse. We attribute the capacity decay to its structural difference with Si-nanopaper. The diameter of the cellulose fibers in regular paper is $\sim 20\ \mu\text{m}$, which is much bigger than the NFC paper, which is $\sim 5\ \text{nm}$. So the Si deposited on regular paper is more like a Si thin film on metal substrates [30]. Therefore, the cycle stability is not as good as Si-conductive nanopaper. In addition, the 3D submicrometer porosity in nanopaper also play important roles in improving the cycle stability.

Conclusions

We have demonstrated nanostructures based on earth-abundant materials using Si and nanocellulose. The performance of the nanostructures is better than that for Si thin film on regular paper substrate. The cost of the conductive

nanopaper could be reduced by replacing CNTs with graphene. The devices demonstrated in this work could be potentially helpful for flexible electronics and low-cost grid-scale storage applications.

Acknowledgement

We acknowledge support from the King Abdullah University of Science and Technology (KAUST) Investigator Award (No. KUS-I1-001-12). We appreciate Erik Garnett's help on the PECVD Si deposition. GZ acknowledges financial support from Agency for Science, Technology and Research (A*STAR). ME and LW acknowledge The Knut and Alice Wallenberg Research Foundation for financial support.

References

- [1] L. Bao, J. Zang, X. Li, *Nano Letters* 11 (2011) 1215-1220.
- [2] A.M. Gaikwad, G.L. Whiting, D.A. Steingart, A.C. Arias, *Advanced Materials* 23 (2011) 3251.
- [3] P.-C. Chen, G. Shen, S. Sukcharoenchoke, C. Zhou, *Applied Physics Letters* (2009) 94.
- [4] H. Nishide, K. Oyaizu, *Science* 319 (2008) 737-738.
- [5] J. Chen, Y. Liu, A.I. Minett, C. Lynam, J. Wang, G.G. Wallace, *Chemistry of Materials* 19 (2007) 3595-3597.
- [6] V.L. Pushparaj, M.M. Shaijumon, A. Kumar, S. Murugesan, L. Ci, R. Vajtai, R.J. Linhardt, O. Nalamasu, P.M. Ajayan, *Proceedings of the National Academy of Sciences of the United States of America* 104 (2007) 13574-13577.
- [7] C. Meng, C. Liu, L. Chen, C. Hu, S. Fan, *Nano Letters* 10 (2010) 4025-4031.
- [8] R.T. Olsson, M.A.S.A. Samir, G. Salazar-Alvarez, L. Belova, V. Strom, L.A. Berglund, O. Ikkala, J. Nogues, U.W. Gedde, *Nature Nanotechnology* 5 (2010) 584-588.
- [9] S. Bourderau, T. Brousse, D.M. Schleich, *Journal of Power Sources* 81 (1999) 233-236.
- [10] J.B. Bates, N.J. Dudney, B. Neudecker, A. Ueda, C.D. Evans, *Solid State Ionics* 135 (2000) 33-45.
- [11] N. Dimov, S. Kugino, M. Yoshio, *Electrochimica Acta* 48 (2003) 1579-1587.
- [12] J. Graetz, C.C. Ahn, R. Yazami, B. Fultz, *Electrochemical and Solid State Letters* 6 (2003) A194-A197.
- [13] U. Kasavajjula, C. Wang, A.J. Appleby, *Journal of Power Sources* 163 (2007) 1003-1039.
- [14] C.K. Chan, H. Peng, G. Liu, K. McIlwrath, X.F. Zhang, R.A. Huggins, Y. Cui, *Nature Nanotechnology* 3 (2008) 31-35.
- [15] L.-F. Cui, L. Hu, J.W. Choi, Y. Cui, *ACS Nano* 4 (2010) 3671-3678.
- [16] A.R. Kamali, D.J. Fray, *Journal of New Materials for Electrochemical Systems* 13 (2010) 147-160.
- [17] N. Liu, L. Hu, M.T. McDowell, A. Jackson, Y. Cui, *ACS Nano* 5 (2011) 6487-6493.
- [18] Y. Yao, M.T. McDowell, I. Ryu, H. Wu, N. Liu, L. Hu, W.D. Nix, Y. Cui, *Nano Letters* 11 (2011) 2949-2954.
- [19] L. Jabbour, C. Gerbaldi, D. Chaussy, E. Zeno, S. Bodoardo, D. Beneventi, *Journal of Materials Chemistry* 20 (2010) 7344-7347.
- [20] J. Zou, J. Liu, A.S. Karakoti, A. Kumar, D. Joung, Q. Li, S.I. Khondaker, S. Seal, L. Zhai, *ACS Nano* 4 (2010) 7293-7302.
- [21] M.B. Bryning, D.E. Milkie, M.F. Islam, L.A. Hough, J.M. Kikkawa, A.G. Yodh, *Advanced Materials* 19 (2007) 661-664.
- [22] J. Fricke, T. Tillotson, *Thin Solid Films* 297 (1997) 212-223.
- [23] W. Bauhofer, J.Z. Kovacs, *Composites Science and Technology* 69 (2009) 1486-1498.
- [24] J.K.W. Sandler, J.E. Kirk, I.A. Kinloch, M.S.P. Shaffer, A.H. Windle, *Polymer* 44 (2003) 5893-5899.
- [25] L. Wagberg, G. Decher, M. Norgren, T. Lindstrom, M. Ankerfors, K. Axnaes, *Langmuir* 24 (2008) 784-795.
- [26] J.N. Coleman, S. Curran, A.B. Dalton, A.P. Davey, B. McCarthy, W. Blau, R.C. Barklie, *Physical Review B* 58 (1998) R7492-R7495.
- [27] L. Hu, H. Wu, Y. Gao, A. Cao, H. Li, J. McDough, X. Xie, M. Zhou, Y. Cui, *Advanced Energy Materials* 1 (2011) 523-527.
- [28] N.-S. Choi, K.H. Yew, K.Y. Lee, M. Sung, H. Kim, S.-S. Kim, *Journal of Power Sources* 161 (2006) 1254-1259.
- [29] R. Ruffo, S.S. Hong, C.K. Chan, R.A. Huggins, Y. Cui, *Journal of Physical Chemistry C* 113 (2009) 11390-11398.
- [30] K.L. Lee, J.Y. Jung, S.W. Lee, H.S. Moon, J.W. Park, *Journal of Power Sources* 129 (2004) 270-274.
- [31] L. Hu, J.W. Choi, Y. Yang, S. Jeong, F. La Mantia, L.-F. Cui, Y. Cui, *Proceedings of the National Academy of Sciences of the United States of America* 106 (2009) 21490-21494.



Liangbing Hu is an assistant professor in Department of Materials Science and Engineering at University of Maryland College Park. He received his B.S. in applied physics from the University of Science and Technology of China (USTC) in 2002. He did his Ph.D. in experimental physics under Prof. George Gruner at UCLA, focusing on carbon nanotube based nanoelectronics. In 2006, he joined Unidym Inc as a co-founding scientist. He worked with Prof. Yi Cui at Stanford University from 2009 to 2011, where he worked on paper and textile energy devices. His research interests include Li-ion batteries, solar cells and printed electronics.



Nian Liu received his B.S. degree in Chemistry from Fudan University in China in 2009, and he is now a graduate student in the Department of Chemistry at Stanford University. His current research involves synthesizing novel nanomaterials and studying their electrochemical properties for high-capacity battery electrode materials.



Martin Eskilsson received his M.S. degree in Bioengineering from Royal Institute of Technology (KTH) in Sweden in 2011 and he is currently a research scientist in Iggesund Paperboard in Sweden. He has been a visiting researcher at Stanford University during 2010-2011. His main research interest is fiber technology.



Guangyuan Zheng received his B.A. degree in Chemical Engineering from University of Cambridge in 2009 and he is currently a graduate student in the Department of Chemical Engineering at Stanford University. His research focuses on developing nanomaterials for energy storage and conversion applications. He has been working on various projects that address the challenges in the high-energy rechargeable batteries systems. He is also interested in utilizing renewable materials for energy applications.



James McDonough received his B.S. degree in chemistry from Harvey Mudd College in Claremont, CA, in 2007, and he is currently a graduate student in the Department of Materials Science and Engineering at Stanford University. His current research involves using nanostructures to improve the performance of energy storage devices, especially supercapacitors and ultracapacitors.



Lars Wågberg is a professor in Fibre Technology at KTH, Royal Institute of Technology at the Department for Fibre and Polymer Technology, in Stockholm, Sweden. He is a member of the Royal Engineering Academia of Sweden. Lars is leading the Fibre Technology team and the work is focused on molecular tailoring of fibres and cellulose fibrils and a fundamental characterization of the colloidal chemical behaviour of cellulose nanofibrils. His focus is also on physical modification methodologies which can be used in aqueous media at neutral pH and room

temperature. High resolution measuring techniques and model surfaces of cellulose is used to clarify the action of polymers and nanoparticles on the properties of fibre and fibril surfaces.



Yi Cui received his B.S. degree in chemistry from the University of Science and Technology of China in 1998 and his Ph.D. in chemistry from Harvard University in 2002. He went on to work as a Miller Postdoctoral Fellow at the University of California, Berkeley. In 2005, he became a professor in the Department of Materials Science and Engineering at Stanford University. He leads a group of researchers working on nanomaterials for energy, electronics and biotechnology. Among other honors, he has received the Wilson Prize from Harvard University (2011), the KAUST Investigator Award (2008), the ONR Young Investigator Award (2008), the MDV Innovators Award (2007) and the Technology Review World Top Young Innovator Award (2004).